Micro-Raman and SEM-EDS analyses to evaluate the nature of salts-cluster particles present in Secondary Marine Aerosol

Héctor Morillas[1], Iker Marcaida[1], Cristina García-Florentino[1], Maite Maguregui[2], Gorka Arana[1] and Juan Manuel Madariaga[1]

[1]Department of Analytical Chemistry, Faculty of Science and Technology, University of the Basque Country UPV/EHU, P.O. Box 644, 48080 Bilbao, Basque Country, Spain
e-mail: hector.morillas@ehu.es
[2]Department of Analytical Chemistry, Faculty of Pharmacy, University of the Basque Country UPV/EHU, P.O. Box 450, 01080 Vitoria-Gasteiz, Basque Country, Spain

ABSTRACT

Marine aerosol is a complex inorganic and organic chemistry system which contains several salts, mainly forming different type of salt clusters. Different environmental parameters have a key role in their formation of these aggregates. The relative humidity (%RH), temperature, CO, SO_2 and NO_x levels and even the O_3 levels (reduction and oxidation) can promote different chemical reactions giving rise to salt clusters with different morphology and sizes. Sulfates, nitrates and chlorides and even chlorosulfates or nitrosulfates are the final compounds which can be found in environments with a direct influence of marine aerosol. In order to collect and analyze these types of compounds, the use of adequate samplers is crucial. In this work, salt-cluster particles were collected thanks to the use of a self-made passive sampler (SMPS) settled in a 20th century historic building (Punta Begoña Galleries, Getxo, Basque Country, Spain) which is surrounded by a beach and a sportive port. These salt-clusters were finally analyzed directly by Raman micro-spectroscopy and scanning electron microscope coupled to an energy dispersive X-ray fluorescence spectroscopy (SEM-EDS).

Keywords: marine aerosol, port environment, Raman spectroscopy, SEM-EDS, dry deposition.

1. Introduction

Marine aerosol constitutes one of the most important natural aerosols from the Earth. It contributes significantly to the Earth's radioactive budget, biogeochemical cycling and even to air quality. Marine aerosol comprises primary and secondary aerosol components. The primary marine aerosol (PMA) is formed due to the interaction of wind with the ocean surface. The result of this interaction is the mechanical production of sea spray (inorganic sea salts and organic matter). Sea spray is produced when the bubbles from the generated whitecap burst. This process originates a jet of saline drops commonly known as sea spray aerosol (SSA). This aerosol carries particles of submicrometre size up to a few micrometres (Rodriguez-Navarro et al., 1999). It is estimated that whitecap formation occurs when the wind reaches the speed of $4\,\mathrm{m\cdot s^{-1}}$. One of the physical characteristics of the sea aerosol is the size of its suspended particles (>1 μm), which depends on the wind speed, sea-air water transfer, etc. (O'Dowd and de Leeuw 2007). The global annual mass emission of primary marine particles (PMP), or sea aerosol, is estimated to range from $2\cdot10^{12}$ to $1\cdot10^{14}$ $\mathrm{Kg\cdot year^{-1}}$, which is comparable to that of dust aerosol (Textor et al., 2006). Apart from this, the SSA has a key role in chemical reactions such as the coupled cycles of sulfate-sea salt (O'Dowd et al., 1999a; 2000) and nitric acid-sea salt (Sørensen et al., 2005). Apart from that, other authors focused their attention in the study of SSA role in the climate change (Intergovernmental Panel on Climate Change (IPCC) In Climate change, 2001). SSA has also been linked to the *marine* boundary layer (MBL) cycle through the activation of halogens, leading to ozone depletion (O'Dowd et al., 1999b; Vogt et al., 1996; McFiggens et al., 2000).

The secondary marine aerosol (SMA) production consists on cluster particle formation resulting from gas to solid particle conversion (O'Dowd and de Leeuw 2007). The sulfur species present in the atmosphere and coming from the anthropogenic emissions are closely related with the SMA formation. The SMA formation occurs in two steps. The first step consists in the new particle formation via the nucleation of 0.5–1 nm stable clusters. Once these clusters are formed, they can grow to larger sizes via condensation. The second step consists in the clusters growing via different heterogeneous reactions and aqueous phase oxidation of dissolved gases in existing aerosol particles. In terms of the sulfur cycle, dimethylsulphide (DMS), a waste produced by phytoplankton, is released from the ocean into the atmosphere where it

undergoes oxidation by the OH radical to form SO_2, which is further oxidized to H_2SO_4 (Charlson et al., 1987). H_2SO_4 is thought to participate in binary homogeneous nucleation with H_2O, and in ternary nucleation with H_2O and NH_3. Apart from this, in coastal zones where regular and significant particle nucleation takes place, iodine oxides have a key role in clusters nucleations and growth (O'Dowd et al., 2002).

According to the different sizes that aerosol particles can raise, marine aerosol clusters can have 1000-10000 nm volume diameter size (Heitzenberg et al., 2003).

Although the main mass fraction of marine aerosol is inorganic sea salts, organic matter is also present and can contribute to the overall mass (Claeys et al., 2010). Usually, marine aerosol carries organic residues from the decomposition of algae, plankton and salts. The most abundant salt carried on marine aerosol is sodium chloride, but other types of chemical compounds like sulfates and nitrates can be also present (Zhao and Gao, 2008; Abdalmogith et al., 2006).

Apart from chlorides, sulfates and nitrates, other ions are also present in a suspended way such as Ca^{2+}, K^{+}, Mg^{2+}, Fe^{3+}, Al^{3+}, Sr^{2+}, NH_4^{+}, HCO_3^{-} and Br^{-}. Usually, organic matter has also high importance because it represents around the 10% of marine aerosol (Chameides and Stelson, 1992; Tervahattu et al., 2005). Additionally, $P.M._{2.5}$ and $P.M._{10}$ airborne particulate matter can be transported by the marine aerosol including metals such as Pb, Cd, Cr, Mn, Cu, Mo, Rh, Ni, As, Ti, V and Hg (Calparsoro et al., 2017; Arruti et al.., 2011; Morillas et al., 2016a; 2016b). The source of these heavy metals can reside in the influence of maritime traffic, port activities and also industry or even road traffic (Gómez et al., 2005).

Taking into account the high amount of cluster-salts present in marine aerosol, it is clear that this environmental factor has influence on the surrounding landscape. One of this is the surrounding built heritage. In this sense, there are many chemical reactions involved in the interaction between marine aerosol and building materials (García-Florentino et al. 2016; Morillas et al. 2012; 2013; 2015a; 2016c; 2016d).

In this work, a marine cluster salts study based on the use of Raman micro-spectroscopy and SEM-EDS was carried out. Thanks to the use of self-made passive sampler (SMPS) settled in a 20^{th} century historic building (Punta Begoña Galleries, Getxo, Basque Country, Spain), which is surrounded by a beach and a sportive port, the salt-clusters

were collected. Moreover, in order to correlate the nature of some cluster salts, different environmental parameters (RH%, Tº(ºC), CO, O_3, SO_x and NO_x) were extracted from Basque Government environmental station which is located close to the sportive port.

2. Materials and methods

2.1 Self-made passive sampler (SMPS)

The passive sampler design used and successfully tested in the Punta Begoña Galleries has been previously described elsewhere (Morillas et al., 2016a). This passive sampler basically consists in a polystyrene cylinder where several pins stubs covered with carbon tapes are inserted inside. Thanks to the natural wind and the nature of the tapes, many different types of suspended particles can be deposited (see Figure 1). The content of the "pin stubs", mainly particulate material adhered to it, can be characterized directly without any pretreatment in the laboratory, which can be considered one of the greater advantages of this sampler, comparing to other systems of particulate matter sampling

2.2 Climate conditions

Thanks to the Basque Government environmental station which is located close to the sportive port, different environmental parameters were extracted (see Figure S1 from Supplementary Material). As it can be seen, the high levels of NO_x and SO_2 during the autumn and winter helped us to decide the best sampling period (from November to February) in order to collect the highest amount of salt-clusters.

2.3 Instrumentation

The SEM-EDS analyses were carried out using an EVO®40 Scanning Electron Microscope (Carl Zeiss NTS GmbH, Germany) coupled to a X-Max Energy-Dispersive X-ray spectrometer (Oxford Instruments, Abingdon, Oxfordshire, United Kingdom) for electron image acquisitions and elemental analysis (punctual and imaging). Although sometimes, deposited particles alone are not conductive, it was possible to obtain optimal results without coating the samples. SEM images were obtained at high vacuum employing an acceleration voltage of 30 kV and a 10 to 400 μm working distance.

Different magnifications (reaching up to ×6800) were used for secondary electron images and an integration time of 50 s was employed to improve the signal-to-noise ratio. The EDS spectra were acquired and treated using the INCA software. Furthermore, a map acquisition of specific microscopic areas in the samples was also performed, allowing the evaluation of the distribution of these elements throughout the sample.

For the micro-Raman analyses, the inVia Renishaw confocal Raman microspectrometer (Renishaw, Gloucestershire, UK) coupled to a DMLM Leica microscope with 5×, 20×, 50×, and 100× long working distance lens was used. Excitation laser (514 nm; nominal laser power 350 mW and 50 mW, respectively) and different magnification lenses (50× and 100×, mainly) were used to perform the measurements. The spectrometer was daily calibrated by using the 520 cm^{-1} Raman band of a silicon chip. Lasers were set at low power (not more than 1 mW at the sample) in order to avoid sample decomposition. Data acquisition was carried out using the Wire 3.2 software package (Renishaw). Spectra were acquired between 100 and 3000 cm^{-1} and several scans (between 10-40 scans) were accumulated for each spectrum in order to improve the signal-to-noise ratio. The interpretation of all the Raman results was performed by comparison of the acquired Raman spectra with Raman spectra of pure standard compounds collected in the e-VISNICH dispersive Raman database (Maguregui et al., 2010). Additionally, free Raman databases (e.g. RRUFF (Downs and Hall-Wallace, 2002)) were also considered for the assignation of Raman bands.

3. Results and Discussion

As mentioned above, the location of the Punta Begoña Galleries makes the façade to be exposed to all types of atmospheric conditions. In this sense, the favorable direction of the winds to the façade is a determining factor in the deposition of the particles. It should also be noted that the presence of the marine aerosol also influences on the composition of the set of suspended particles and cluster salts, which in turn have a negative influence on the durability of the materials.

3.1 SEM-EDS analyses

The results obtained by SEM-EDS indicated the presence of salts with different elemental composition. Indeed, as shown in Figure 2, different acquired mappings and subsequently their elemental distribution is presented in the cluster salt itself. Usually, the elemental base is Halite (NaCl) and around of this, different particles can be observed in which their composition can vary (see Figure 2A, 2B, 2C and 2D). Thus, as can be seen in Figures 2A and 2B, the elemental composition of Ca, S and O could be related to the presence of calcium sulfates (anhydrite ($CaSO_4$) and/or gypsum ($CaSO_4 \cdot 2H_2O$)). Additionally, other elements such as Mg, K, and Si may be also related to the presence of aluminosilicates and other types of sulfates such as magnesium sulfates (epsomite ($MgSO_4 \cdot 7H_2O$) and hexahydrite ($MgSO_4 \cdot 6H_2O$)). Moreover, as shown in Figure 2C, other elements such as nitrogen are also present, which may be related to the presence of nitrates coupled to halite particles. The fact that these particles are present in this environment demonstrates how aggressive the environment is for the conservation of the Galleries under study. On the other hand, the presence of other additional elements such as phosphorus and fluor was observed (see Figure 2D), which would be directly related to the presence of phosphate compounds which are in the environment and easily coupled to these halite particles. Finally, the presence of fluor couldbe related with the presence of fluorides, compounds that are usually present in the marine aerosol. All of these compounds as it has been pointed out above, have a degradation effect on building materials, causing the formation of salts and over time promoting loss of material.

In many cases, different salts present in the atmosphere react with other salts giving rise to new compounds that can grow till larger sizes depending on the different atmospheric conditions. Temperature, pressure and relative humidity (% RH) play a key role in this type of reactions. Thus, during time, these salts can grow giving rise to clusters of salts that can react with the building material through dry deposition, promoting reactions on the material itself, and causing over time the loss of material. As an example, in Figure 3, the process of formation of a mixed sulfate ($NaCaClSO_4$) can be observed. In this way, through reactions between halite (NaCl, the most common salt in the marine aerosol) (Figure 3A) together with anhydrite ($CaSO_4$) (Figure 3B) also present in the sea salt can lead to the complex $NaCaClSO_4$ (Figure 3D). This reaction process has been observed in the Punta Begoña SMPS. In addition, it was possible to be observe in an intermediate step how the halite and anhydrite particles are mixed together to form that

complex (Figure 3C). In the following reactions (1-3) the possible formation of the $NaCaClSO_4$ is presented.

$$CaSO_4 \cdot 2H_2O\ (s) \leftrightarrows Ca^{2+}\ (aq) + SO_4^{2-}\ (aq) + 2H_2O\ (l) \quad (1)$$

$$NaCl\ (s) \leftrightarrows Na^{+}\ (aq) + Cl^{-}\ (aq) \quad (2)$$

$$Na^{+}\ (aq) + Cl^{-}\ (aq) + Ca^{2+}\ (aq) + SO_4^{2-}\ (aq) \leftrightarrows NaCaClSO_4\ (s) \quad (3)$$

In addition, as it can be seen in Figure 4, cluster salts such as glauberite ($Na_2Ca(SO_4)_2$) were also identified in the marine aerosol, which appeared in the Punta Begoña Galleries sampling point with great assiduity (Figure 4A). Thus, related with this compound and as shown in Figure 4B, different particles composed by aluminosilicates and iron oxides can be added to glauberite, increasing its cluster salt diameter size (up to 60 μm). In the same way, halite particles and other conglomerates such as iron oxides and aluminosilicates can be coupled together, forming consequently more complex compounds or clusters (Figure 4C).

3.2 Raman spectroscopy analyses

To complement the elemental information obtained by SEM-EDS, Raman analyses of the salts deposited in the pins placed in the Punta Begoña Galleries were directly carried out, in where the molecular composition of these salts clusters was obtained. Micro-Raman spectroscopy revealed the presence of many cluster salts, which during time can react with the Punta Begoña Galleries materials by dry deposition, giving rise to different decay processes that can promote loss of material. In general way, a summary table of the main salts-clusters detected by Raman spectroscopy is presented (see Table 1). As it can be observed in Table 1, the great majority of the compounds identified corresponds to sulfates, which corroborates the observed results obtained by SEM-EDS, where magnesium sulfates (hexahydrite, epsomite), calcium sulfates (anhydrite and gypsum), as well as all kinds of mixed and complex sulfates such as eugsterite, syngenite, polyhalite and glauberite were also observed. In addition to this massive presence of sulfates, the presence of nitrates such as nitratine and mixed compounds such as darapskite are also observed. In this case as explained above, sulfates and nitrates have a degrading effect on the materials.

Moreover, as example, different Raman spectra of these clusters are also presented in the Figure 5. In this way, mascagnite ($(NH_4)_2SO_4$), main raman band at 974 cm^{-1}) (Morillas et al., 2015b) (Figure 5A), nitratine ($NaNO_3$, main raman band at 1067 cm^{-1}) (Morillas et al., 2016e) (Figure 5B), epsomite ($MgSO_4 \cdot 7H_2O$, main raman band at 985 cm^{-1}) (Figure 5C) and syngenite ($K_2Ca(SO_4) \cdot H_2O$) (Morillas et al., 2015b) main raman bands at 981 and 1006 cm^{-1}) (Figure 5D) were observed. Other cluster salts such as niter (KNO_3), glauberite ($CaNa_2(SO_4)_2$), anhydrite ($CaSO_4$) and hexahydrite ($MgSO_4 \cdot 6H_2O$) were also observed.

4. Conclusions

The combined analytical methodology used in this work using SEM-EDS (point by point and imaging) and Raman spectroscopy has been proved as a powerful analytical strategy to characterize the composition of different salt-clusters particles from the SMA. The different climatic conditions (%RH, T^o, CO, O_3, NO_x and SO_2) showed that the period from November to February () is the best one to perform the sampling due to higher levels of NO_x and SO_2. The SMPS presented in this work has been proved as a powerful, cheap and efficient system that helped us to characterize the different cluster salts present in marine aerosol and that can be deposited on the surface of building materials by dry deposition process. The deposited particles can react with Built Heritage material, promoting the formation of deterioration products that during time jeopardize the loss of material in the building. Finally, in this work, the influence of marine aerosol in the conservation state of historical buildings has been demonstrated, where these particles such as sulfates and nitrates cannot be only formed in the building material following a reaction between the carbonate from the material itself and the acid aerosols deposited following wet deposition, but also by the inclusion of salts coming from water infiltrations, as it has been described in the literature many times. The sulfate, nitrate and chloride salts can also be present in the material as deposited airborne particulate matter following dry deposition.

Acknowledgements

This work has been funded by the Ministry of Economy and Competitiveness and the European Regional Development Fund (ERDF) through the project DISILICA-1930 (ref. BIA2014-59124-P) and by the cooperation agreement between the University of the Basque Country (UPV/EHU) and the City Council of Getxo (OTRI2014-0639). Technical support provided by General X-ray Service of the SGIKer (UPV/EHU, Ministry of Economy and Competitiveness of Spain, Basque Government, ERDF and European Social Fund) is also gratefully acknowledged.

References

Abdalmogith, S.S., Harrison, R.M., Derwent, R.G., 2006. Particulate sulphate and nitrate in Southern England and Northern Ireland during 2002/3 and its formation in a photochemical trajectory mode, Science of the Total Environment. 368, 769-780.

Arruti, A., Fernandez-Olmo, I., Irabien, A., 2011. Regional evaluation of particulate matter composition in an Atlantic coastal area (Cantabria region, northern Spain): Spatial variations in different urban and rural environments, Atmospheric Research. 101, 280-293.

Calparsoro, E., Maguregui, M., Giakoumaki, A., Morillas, H., Madariaga, J.M., 2017. Evaluation of black crust formation and soiling process on historical buildings from the Bilbao metropolitan area (north of Spain) using SEM-EDS and Raman microscopy, Environ. Sci. Pollut. Res. 24, 9468–9480.

Chameides, W.L., Stelson, A.W., 1992. Aqueous-phase chemical processes in deliquescent sea salt aerosols: A mechanism that couples the atmospheric cycles of S and sea salts, Journal of Geophysical Research. 97, 565-580.

Charlson, R.J., Lovelock, J.E., Andreae, M.O., Warren, S.G., 1987. Oceanic phytoplankton, atmospheric sulfur, cloud albedo and climate, Nature. 326, 655–661.

Claeys, M., Wang, W., Vermeylen, R., Kourtchev, I., Chi, X., Farhat, Y., Surratt, J.D., Gómez-González, Y., Sciare, J., Maenhaut, W., 2010. Chemical characterisation of

284 marine aerosol at Amsterdam Island during the austral summer of 2006–2007, Journal
285 of Aerosol Science. 41, 13-22

286 Downs, R.T., Hall-Wallace, M., 2002. A database of crystal structures published in the
287 American mineralogist and the Canadian mineralogist and its use as a resource in the
288 classroom. 18th General Meeting of the International Mineralogical Association, p. 128.

289 García-Florentino, C., Maguregui, M., Morillas, H., Balziskueta, U., Azcarate, A.,
290 Arana, G., Madariaga, J.M., 2016. Portable and Raman imaging usefulness to detect
291 decaying on mortars from Punta Begoña Galleries (Getxo, North of Spain), J. Raman
292 Spectrosc. 47, 1458–1466.

293 Gómez, E.T., Sanfeliu, T., Rius, J., Jordan, M.M., 2005. Evolution, Sources and
294 Distribution of Mineral Particles and Amorphous Phase of Atmospheric Aerosol in An
295 Industrial and Mediterranean Coastal Area, Water Air & Soil Pollution. 167, 311-330.

296 Heintzenberg, J., Raes, F., Schwartz, S., Atmospheric Chemistry in a Changing World,
297 Chapter 4. Tropospheric Aerosols, Springer-Verlag, New York, USA, (2003).

298 Intergovernmental Panel on Climate Change (IPCC) In Climate change 2001: the
299 scientific basis (eds J. T. Houghton, Y. Ding, D. J. Griggs, M. Noguer, P. J. van der
300 Linden & D. Xiaosu), Cambridge University Press, New York, USA, 2001.

301 Maguregui, M., Prieto-Taboada, N., Trebolazabala, J., Goienaga, N., Arrieta, N.,
302 Aramendia, J., Gomez-Nubla, L., Sarmiento, A., Olivares, M., Carrero, J.A., Martinez-
303 Arkarazo, I., Castro, K., Arana, G., Olazabal, M.A., Fernandez, L.A., Madariaga, J.M.,
304 2010. CHEMCH 1st International Congress Chemistry for Cultural Heritage, Ravenna,
305 30th June–3rd July.

306 McFiggens, G., Plane, J.M.C., Allan, B.J., Carpenter, L.J., Coe, H., O'Dowd, C.D.,
307 2000. A model study of Iodine chemistry in the marine boundary layer, Journal of
308 Geophysical Research. 105, 14371-14386.

309 Morillas, H., Maguregui, M., Gómez-Laserna, O., Trebolazabala, J., Madariaga, J.M.,
310 2012. Characterisation and diagnosis of the conservation state of cementitious materials
311 exposed to the open air in XIX century lighthouses located on the coast of the Basque

312 Country: “the case of Igueldo lighthouse, San Sebastian, North of Spain”. J. Raman
313 Spectrosc. 43, 1630–1636.

314 Morillas, H., Maguregui, M., Gómez-Laserna, O., Trebolazabala, J., Madariaga, J.M.,
315 2013. Could marine aerosol contribute to deteriorate building materials from interior
316 areas of lighthouses? An answer from the analytical chemistry point of view. J. Raman
317 Spectrosc. 44, 1700–1710.

318 Morillas, H., Maguregui, M., Paris, C., Bellot-Gurlet, L., Colomban, P., Madariaga,
319 J.M., 2015a. The role of marine aerosol in the formation of (double) sulphate/nitrate
320 salts in plasters. Microchem. J. 123, 148–157.

321 Morillas, H., Maguregui, M., Trebolazabala, J., Madariaga, J.M., 2015b. Nature and
322 origin of white efflorescence on bricks, artificial stones, and joint mortars of modern
323 houses evaluated by portable Raman spectroscopy and laboratory analyses.
324 Spectrochim. Acta A-M. 136, 1195–1203.

325 Morillas, H., Maguregui, M., García-Florentino, C., Marcaida, I., Madariaga, J.M.,
326 2016a. Study of particulate matter from Primary/Secondary Marine Aerosol and
327 anthropogenic sources collected by a self-made passive sampler for the evaluation of the
328 dry deposition impact on Built Heritage, Sci. Total Environ. 550, 285-296.

329 Morillas, H., Maguregui, M., García-Florentino, C., Carrero, J.A., Salcedo, I.,
330 Madariaga J.M., 2016b. The cauliflower-like black crusts on sandstones: A natural
331 passive sampler to evaluate the surrounding environmental pollution, Environ. Res. 147,
332 218-232.

333 Morillas, H., García-Galan, J., Maguregui, M., García-Florentino, C., Marcaida, I.,
334 Carrero, J.A., Madariaga, J.M., 2016c. In-situ multianalytical methodology to evaluate
335 the conservation state of the entrance arch of La Galea Fortress (Getxo, north of Spain),
336 Microchem. J. 128, 288-296.

337 Morillas, H., García-Galán, J., Maguregui, M., Marcaida, I., García-Florentino, C.,
338 Carrero, J.A., Madariaga, J.M., 2016d. Assessment of marine and urban-industrial
339 environments influence on built heritage sandstone using X-ray fluorescence
340 spectroscopy and complementary techniques, Spectrochim. Acta B. 123, 76-88.

Morillas, H., Marcaida, I., Maguregui, M., Carrero, J.A., Madariaga, J.M., 2016e. The influence of rainwater composition on the conservation state of cementitious building materials, Sci. Total Environ. 542, 716-727.

O'Dowd, C.D., Lowe, J.A., Smith, M.H., 1999a. Coupling sea-salt and sulphate interactions and its impact on predicting cloud droplet concentrations, Geophysical Research Letters. 26, 1311-1314.

O'Dowd, C.D., Lowe, J.A., Smith, M.H., Kaye, A.D., 1999b. The relative importance of sea-salt and nss-sulphate aerosol to the marine CCN population: an improved multi-component aerosol-droplet parameterization, Quarterly Journal of the Royal Meteorological Society. 125, 1295-1313.

O'Dowd, C.D., Lowe, J.A., Clegg, N, Clegg, S.L., Smith, M.H., 2000. Modelling heterogeneous sulphate production in maritime stratiform clouds, Journal of Geophysical Research. 105, 7143-7160.

O'Dowd, C.D., Hämeri, K., Mäkela, J.M., Pirjola, L., Kulmala, M., Jennings, S.G., Berresheim, H., Hansson, H.C., de Leeuw, G., Kunz, G.J., Allen, A.G., Hewitt, C.N., Jackson, A., Viisanen, Y., Hoffmann, T., 2002. A dedicated study of new particle formation and fate in the coastal environment (PARFORCE): overview of objectives and initial achievements, Journal of Geophysical Research. 107, 8108.

O'Dowd, C.D., de Leeuw, G., 2007. Marine aerosol production: a review of the current knowledge, Philosophical Transactions of Royal Society A. 365, 1753-1774.

Rodriguez-Navarro, C., Doehne, E., Sebastian, E., 1999. Origins of honeycomb weathering: The role of salts and wind, GSA Bulletin. 111, 1250-1255.

Sørensen, L.L., Pryor, S., de Leeuw, G., Schulz, M., 2005. Flux divergence for nitric acid in the marine atmospheric surface layer, Journal of Geophysical Research. 110, D15306.

Tervahattu, H., Juhanoja, J., Vaida, V., Tuck, A.F., Niemi, J.V., Kupiainen, K., Kulmala, M., Vehkamäki, H., 2005. Fatty acids on continental sulfate aerosol particles, Journal of Geophysical Research-Atmospheric. 110, 1984-1991.

Textor, C., Schulz, M., Guibert, S., Kinne, S., Balkanski, Y., Bauer, S., Berntsen, T., Berglen, T., Boucher, O., Chin, M., Dentener, F., Diehl, T., Easter, R., Feichter, H., Fillmore, D., Ghan, S., Ginoux, P., Gong, S., Kristjansson, J.E., Krol, M., Lauer, A., Lamarque, J.F., Liu, X., Montanaro, V., Myhre, G., Penner, J., Pitari, G., Reddy, S., Seland, O., Stier, P., Takemura, T., Tie, X., 2006. Analysis and quantification of the diversities of aerosol life cycles within AeroCom, Atmospheric Chemistry and Physics. 6, 1777-1813.

Vogt, R., Crutzen, P.J., Sander, R., 1996. A mechanism for halogen release from sea salt aerosol in the remote marine boundary layer, Nature. 383, 327-330.

Zhao, Y., Gao, Y., 2008. Acidic species and chloride depletion in coarse aerosol particles in the US east coast, Science of the Total Environment. 407, 541-547.

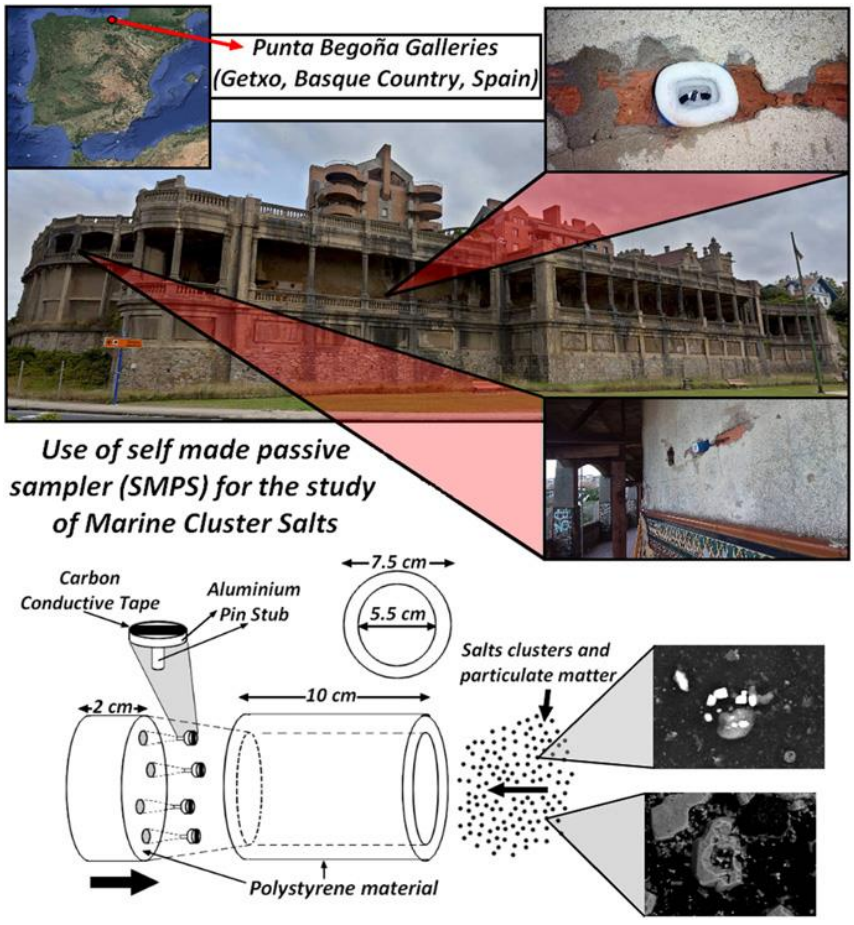

Figure 1 Fig. 1. a) Scheme of the Punta BegoñaGalleries sampling and b) self-made passive sampler (SMPS) scheme.

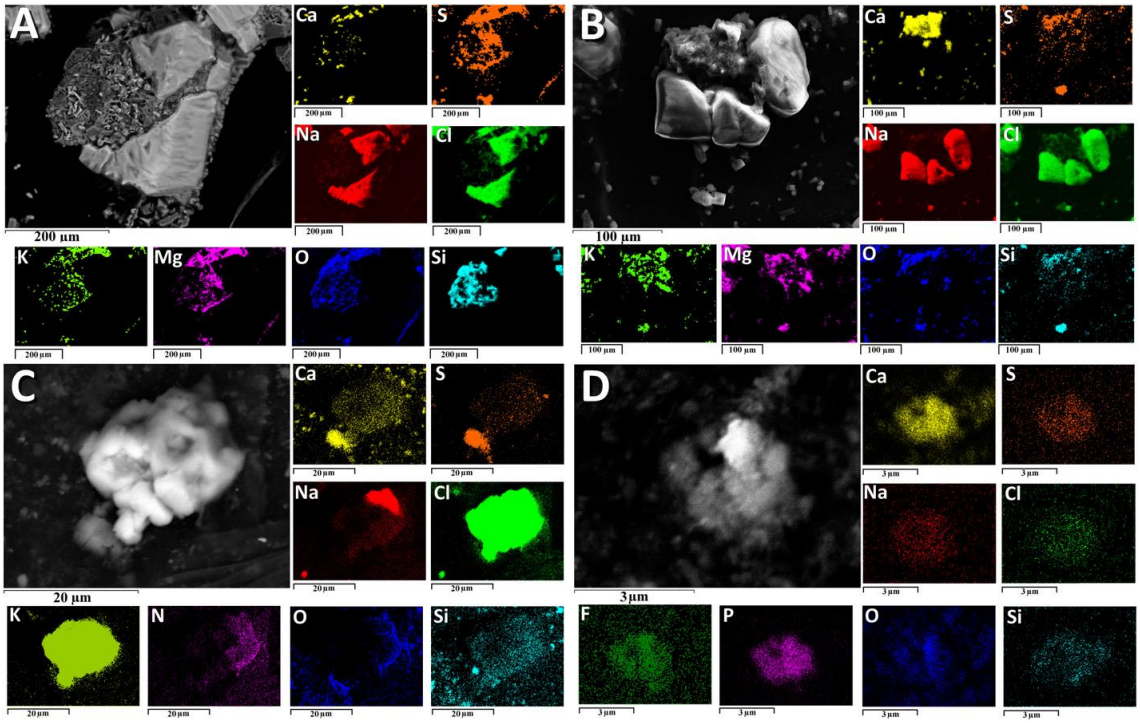

384

385 Figure. 2. SEM-EDS imaging showing in all the figures the major presence of Na and
386 Cl and around themA) and B) Ca, S and O (calcium sulfates presence) and Mg, K, and
387 Si (aluminosilicates and sulfates presence) distributions; C) N and O (possible nitrates
388 presence) distributions and D) P and F distributions (possible phosphate and fluoride
389 presence).

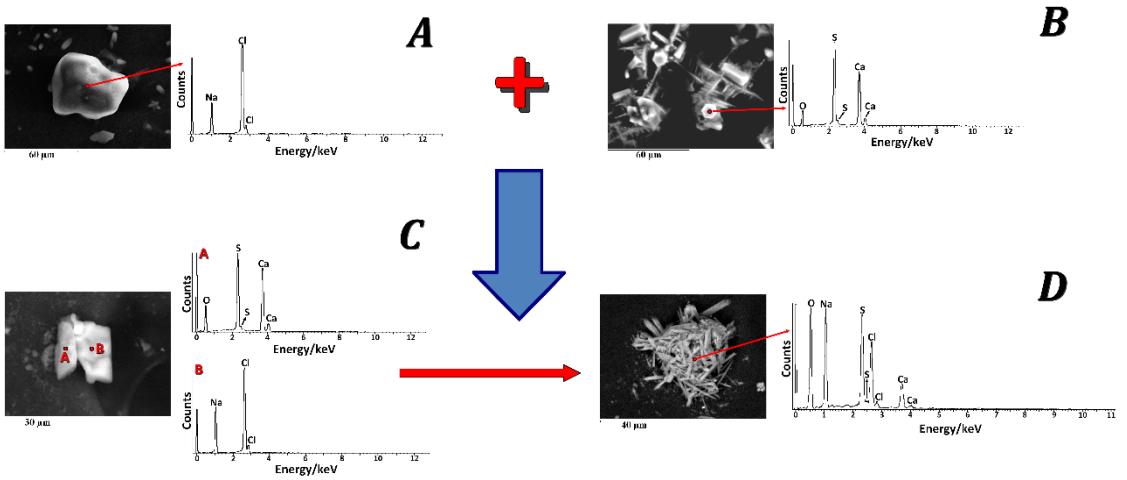

390

391 Figure 3. Process of formation of the mixed sulfate-chloride NaCaClSO4 showing the
392 different reaction steps that lead to its formation starting from A) halite (NaCl) and B)
393 calcium sulfate (anhydrite, $CaSO_4$ and/or gypsum, $CaSO_4 \cdot 2H_2O$); C) intermediate salt
394 cluster formation and D) final $NaCaClSO_4$ formation.

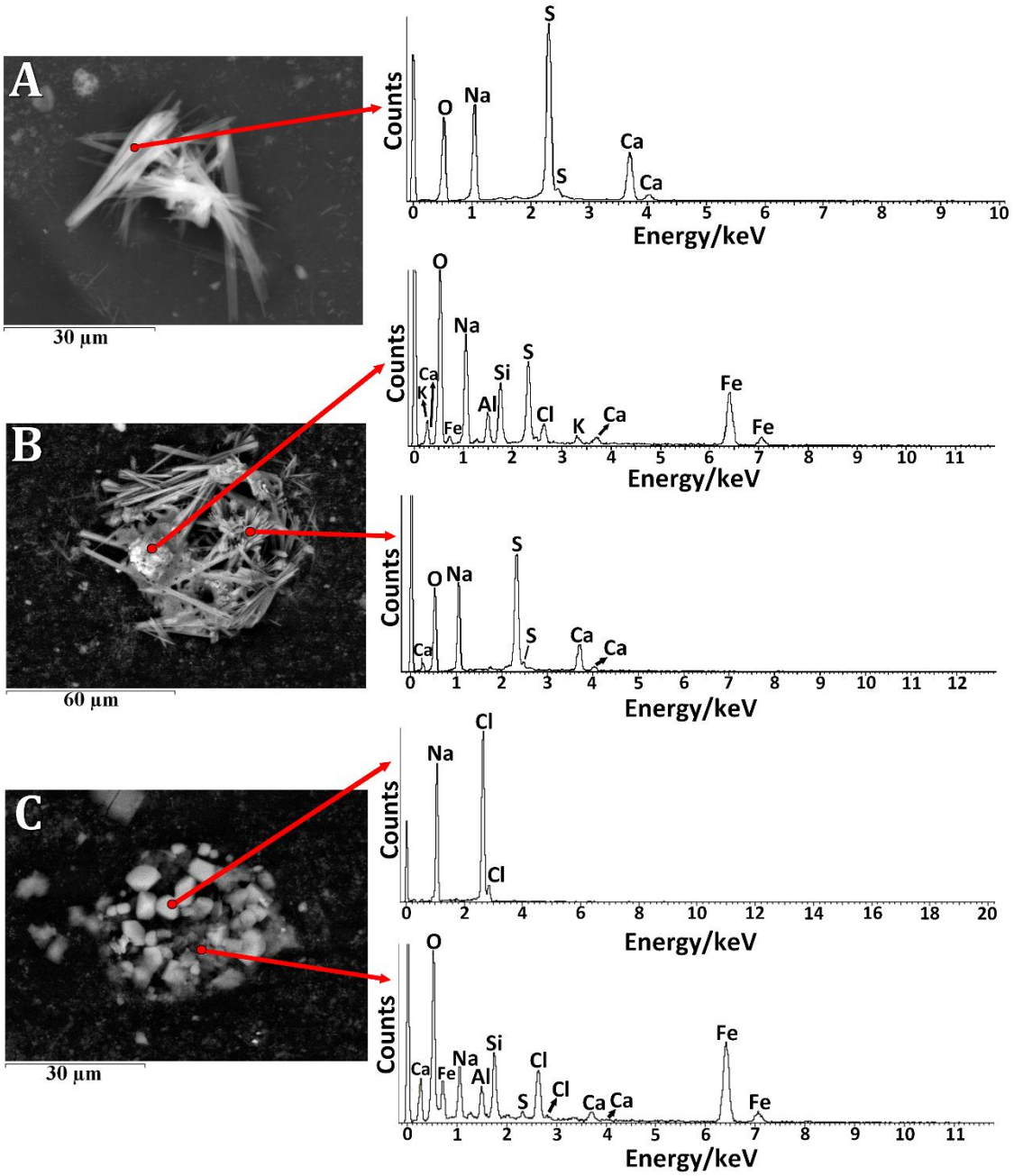

Figure 4. Different SEM-EDS results of salt clusters composed by A) Ca, Na, S and O (possible glauberite NaCaSO4) of diameter size up to 30 µm, B) aluminosilicates and iron oxides added to possible glauberite with diameter size up to 60 µm and C) Na and Cl (halite, NaCl) composed salt cluster (diameter size up to 30 µm) which includes elements such as Al, Si, Fe and Ca.

Table 1. Raman spectra of the salts-cluster particles

Salts-Cluster particles	***Mineral Name***	***Raman bands ν (cm^{-1})***
$CaSO_4$	Anhidrite type III	420 m, 490m, 630m, 673m, 1025 vs, 1167m.
$Na_3(SO_4)(NO_3)\cdot H_2O$	Darapskite	472 vw, 619 w, 640 w, 707 w, 729 w, 993 s, 1059 vs, 1084 w, 1122 vw, 1354 w, 1416 w.
$Na_4Ca(SO_4)_3\cdot H_2O$	Eugsterite	1084 s, 1124 s
$K_2Ca(SO_4)\cdot H_2O$	Syngenite	441 s, 472 m, 492 w, 603 m, 621 m, 633 m, 642 m, 661 m, 981 vs, 1006 vs, 1082 m, 1119 m, 1139 w, 1165 w.
$K_2Ca_2Mg(SO_4)_4\cdot 2H_2O$	Polyhalite	236 m, 438 m, 465 s, 623 vw, 653 m, 989 vs, 1016 vs, 1071 m, 1093 m, 1131 m, 1165 m.
$CaNa_2(SO4)_2$	Glauberite	453 w, 471 s, 485 m, 619 m, 624 m, 636 m, 644 s, 1001 vs, 1106 w, 1139 s, 1156 m, 1169 m
$(NH_4)_2SO_4$	Mascagnite	449 m, 614 w, 622 w, 974 vs, 1104 vw, 1417 vw.
$CaSO_4\cdot 2H_2O$	Gypsum	413 m, 492 m, 619 m, 673 m, 1008 vs, 1132 m.
K_2SO_4	Arcanite	455 m, 619 m, 988 vs, 1092 w, 1103 w, 1144 vw.
$MgSO_4\cdot 6H_2O$	Hexahydrite	249 w, 361 w, 442 w, 464 vw, 603 w, 982 vs, 1083 vw, 1148 vw.
$MgSO_4\cdot 7H_2O$	Epsomite	362 vw, 445 w, 462 w, 609 w, 985 vs, 1082 vw, 1145 vw.
Na_2SO_4	Thenardite	450 w, 465 w, 621 m, 632 m, 647 m, 992 vs, 1101 m, 1132 m, 1152 m.
$Na_2SO_4\cdot 10H_2O$	Mirabilite	446 w, 458 w, 616 m, 628 m, 989 vs, 1108 m, 1120 m, 1130m.
$NaNO_3$	Nitratine	188 m, 414 vw, 518 vw, 533 vw, 722 s, 1067 vs, 1383 w, 1663 vw, 1775 vw.
$Mg(NO_3)_2$	Nitromagnesite	729 s, 1059 vs, 1359 m, 1432 w.